CONF-790610--5

PHOTON SCATTERING BY THE GIANT DIPOLE RESONANCE

by

T.J. Bowles, R.J. Holt, H.E. Jackson, R.D. McKeown, and J.R. Specht

Prepared for

International Conference

on

Nuclear Physics with Electromagentic Interactions

Mainz, Germany

June 5-9, 1979

U of C-AUA-USDOE

ARGONNE NATIONAL LABORATORY, ARGONNE, ILLINOIS

Operated under Contract W-31-109-Eng-38 for the

U. S. DEPARTMENT OF ENERGY

cap

DISCLAIMER

The facilities of Argonne National Laboratory are owned by the United States Government. Under the terms of a contract (W-31-109-Eng-38) among the U. S. Department of Energy, Argonne Universities Association and The University of Chicago, the University employs the staff and operates the Laboratory in accordance with policies and programs formulated, approved and reviewed by the Association.

MEMBERS OF ARGONNE UNIVERSITIES ASSOCIATION

The University of Arizona
Carnegie-Mellon University
Case Western Reserve University
The University of Chicago
University of Cincinnati
Illinois Institute of Technology
University of Illinois
Indiana University
Iowa State University
The University of Iowa
Kansas State University
The University of Kansas
Loyola University
Marquette University
Michigan State University
The University of Michigan
University of Minnesota
University of Missouri
Northwestern University
University of Notre Dame
The Ohio State University
Ohio University
The Pennsylvania State University
Purdue University
Saint Louis University
Southern Illinois University
The University of Texas at Austin
Washington University
Wayne State University
The University of Wisconsin

The giant dipole resonance is one of the simplest and most basic features of nuclear matter. It was discovered in the earliest days of nuclear physics and since has been studied in the greatest detail. We know many of its features with some precision but there are still basic aspects of its character which are poorly understood. One of these is the coupling between the basic dipole oscillation and other nuclear collective degrees of freedom such as surfaced vibrations and rotations. Elastic and inelastic photon scattering is an ideal probe for studying this feature of the giant dipole resonance. The basic photon interaction is well known and one can use dispersion relations to connect elastic scattering and photo absorption cross sections. As we will see, the strength of inelastic scattering gives a direct measure of the coupling to collective degrees of freedom such as surface vibrations.

We know in the simple hydrodynamic model[1] that the energy of the dipole resonance is inversely proportional to the nucleus radius:

$$E_{dip} = k/R \approx 80\ A^{-1/3} .$$

However, in a spherical nucleus:

$$R = R_o(1 + \Sigma\, \alpha_{2m} Y^2_m)$$

The surface undergoes a deformation which varies in time according to the equation:

$$\alpha_{2m} = \alpha^{0}_{2m} e^{i\omega t},$$

that is, the nuclear surface undergoes dynamic collective quadrupole vibrations. As a result, one expects a coupling to exist between the giant dipole resonance and surface vibrations in spherical nuclei. In the absence of this coupling, photon scattering through the giant dipole resonance would be purely elastic. The presence of such coupling produces inelastic scattering to low-lying excited states and the photon scattering should provide one of the most sensitive means of observing this coupling. The model most frequently used to esimate the strength of this coupling is the dynamic collective model[2]. For spherical nuclei in the mass 60 range the theory typically predicts an inelastic scattering component about 0.3 of the elastic scattering cross section.

In the dynamic collective model, the giant dipole resonance is treated as a collective density oscillation of proton fluids against neutron fluids as in the hydrodynamic model. Quadrupole surface vibrations are treated in the usual harmonic collective model. A harmonic approximation is used and excitations are treated as coupled oscillators following a Hamiltonian of the form:

$$H = H_{dip} + H_{quad} + H_{dip.quad}$$

It is noted that the characteristic period for surface vibrations is about $\hbar/1$ MeV while the characteristic period for the giant dipole state is $\hbar/15$ MeV indicating that the quadrupole vibrations are very much slower than the giant dipole oscillations. Consequently, the adiabatic approximation can be used to evaluate the coupling constants in the coupling term in the Hamiltonian. These coupling constants are then used in a Hamiltonian which is diagonalized in the basis of the states appropriate to the uncoupled Hamiltonian. The theory predicts two physical effects: first a broadening of the absorption cross section. To date it has been this feature of the absorption cross section which has been used to estimate the strength of the coupling between the giant dipole resonance and other excitations. However, because of the intrinsic width of the dipole state, interpretations of the broadening are relatively difficult. The second effect predicted by the dynamic collective model is a non-zero nuclear tensor polarizability which gives rise to inelastic scattering to the low-lying vibrational states, 0^+ and 2^+ states in even-even targets.

Experimental observation of this inelastic scattering has been hampered by lack of intense monochromatic photon beams. Previous measurements with monochromatic photons have been limited to lower energy regions accessible with reactor-generated photon beams[3]. Two developments have made new measurements possible. The development of large volume high resolution NaI(tℓ) spectrometers has made possible the resolution of elastic and inelastic scattering for monochromatic incident photons. The availability of monochromatic photons from the tagged photon source[4] of the University of Illinois microtron has made possible measurements with incident beams of quasi-monochromatic photons. The experimental arrangement for our measurements are shown in Fig. 1. A beam of electrons from the

Illinois superconducting microtron strike an aluminum converter. The bremsstrahlung produced irradiates a 200 gram sample of ^{60}Ni. Photons are observed in a large volume NaI(tℓ) spectrometer in coincidence with the residual electrons which are magnetically analyzed with the resolution of 150 keV. The electron spectrometer contains an array of 12 detectors permitting simultaneous measurements of a band of photon energies typically of about 4 MeV.

Measurements were made over the range of 15— 22 MeV. For each energy, the elastic and inelastic scattering to the ground states and low-lying excited states was obtained by fitting the spectra of scattered photons with measured line shapes. Figure 2 shows the scattered photon spectrum observed for a ^{60}Ni target at a photon scattering angle of 120° and an incident photon energy of 19.8 MeV. In general we see no scattering to the higher excited states and the inelastic scattering to the first excited 2^+ state is very weak.

Figure 3 shows the results of our first measurements of ^{60}Ni. Plotted is the elastic cross section as well as the total inelastic cross section for a scattering angle of 120°. The solid curve and the dotted curves bound the region on which the scattering cross section was estimated to lie on the basis of information available on the total absorption cross section in ^{60}Ni. The inelastic scattering was found to be surprisingly weak. Over the full energy interval of 15— 22 MeV, the ratio was roughly constant at a value of about 15%. This is in contrast to our expectation that the inelastic scattering would be about 30% of the elastic scattering.

In interpreting the elastic scattering cross sections, it is important to remember that the nuclear resonance elastic scattering is coherent with Thomson scattering and that there is a strong interference asymmetry induced

by this interference. Figure 4 indicates the effect of the Thomson scattering interference. Shown are curves which fit the observed elastic scattering cross section and those same cross sections with the Thomson scattering amplitude removed. It is evident that the effect of Thomson scattering is by no means negligible. Unfortunately many of the calculations of elastic and inelastic scattering in the literature are made without the inclusion of Thomson scattering. And so in the analysis, it is necessary to remove the effect.

Although we know in general that it will not be adequate, for the purposes of data analysis we have assumed that the giant dipole state in nuclei under study can be described in terms of a superposition of two Lorentzian peaks. A two-Lorentzian model offers two advantages. First, it permits a direct comparison with the predictions of a theory due to Kerman and Quang[5] which was introduced as a first attempt to describe the coupling of the giant dipole resonance to surface vibrations. This theory predicts that the elastic and inelastic scattering will result from a superposition of at most three Lorentzian scattering amplitudes. Secondly, the two-Lorentzian formalism offers a convenient way of making a qualitative comparison with the DC collective model particularly since it offers a convenient way of removing the effect of Thomson scattering from the measured cross sections. Figure 5 shows our data for elastic and inelastic scattering by ^{60}Ni fit using this two Lorentzian analysis. The curves represent the best fit to the elastic scattering data and a best fit for the inelastic scattering which uses the resonance parameters which result from the fit to the elastic scattering together with energy-independent branching ratios for each Lorentzian. The best fit Lorentzian parameters are shown in Table I. The branching ratio determined for the inelastic scattering was observed to be 0.14 for the lower Lorentzian and 0.30 for the upper Lorentzian.

Figure 6 shows a comparison of the elastic and inelastic scattering inferred from our analysis with the predictions of the dynamic collective model for the same target. In this case, the observed Lorentzian parameters have been used to generate the cross section at 135° where the theoretical calculations were carried out. Unfortunately, no calculations have been done for ^{60}Ni and so the comparison made is between ^{58}Ni for which calculations exist[6] and our measurements for ^{60}Ni. However, in as much as the properties of the low-lying excitations very similar in ^{58}Ni and ^{60}Ni, we expect the behavior of ^{58}Ni and ^{60}Ni to be roughly the same. It is evident from the spectrum that the experimental data is very different in trend from those obtained from the dynamic collective model calculations. The elastic scattering cross section does not have the shape predicted theoretically and the inelastic scattering is observed to be very much weaker and less peaked than the model calculations indicated.

The second target studied in this mass region was ^{52}Cr. The cross sections measured at 90° are shown in Fig. 7 together with the best fit we were able to obtain using the two Lorentzian analysis. It is evident from an examination of the elastic scattering cross section that there is structure in the elastic scattering which cannot be reproduced in detail by the analysis. Again, the inelastic scattering is observed to be very weak. In this case, we can make a direct comparison between measurement and calculation[6] as is shown in Fig. 8. Again the two-Lorentzian decomposition of data taken at 90° has been used to generate the scattering cross sections which are appropriate to the theoretical calculations carried out at 135°. Again there is little similarity between the experimental shape for the elastic scattering and the theoretically predicted elastic scattering cross section and

again the inelastic scattering is very much weaker than the scattering predicted theoretically and does not show the structure evident in the model calculation.

In order to be certain that our failure to observe significant inelastic scattering strength was not a result of an instrumental problem. We searched for a nucleus in this mass region for which inelastic scattering should be observable with certainty. ^{56}Fe is known to be a rotational nucleus and it is well established from photon scattering measurements at lower energy that there should be a strong inelastic scattering to low-lying rotational levels in a nuclear rotator[7]. Figure 9 shows a typical scattered photon spectrum resulting from our observations of scattering in ^{56}Fe at 90°. We were relieved to observe a strong inelastic scattering component in ^{56}Fe with a strength characteristic of a rotational nucleus. The elastic and inelastic scattering cross sections are shown in Fig. 10 together with the best least squares fits we were able to obtain using the two Lorentzian analysis. It is evident from inspection of the figure that the elastic scattering shows structure which is incompatable with a two-Lorentzian cross section. The sharp peak in the elastic scattering was checked for reproducibility in a second series of measurements. The inelastic scattering was observed to be quite large, particularly at lower energies as is expected for a nuclear rotator. This data gives us confidence that in fact we have the sensitivity to inelastic scattering that our calibrations of the photon spectrometer would indicate.

There have been suggestions in the literature that the mass 60 mass region may be too light a region for the dynamic collective model to be applicable. In particular the neutron structure of ^{52}Cr and the proton structure of ^{60}Ni correspond to a closed $n = 28$ shell. In addition, one expects that isospin effects

may be significant in this mass region. Consequently, in order to find targets that would be more appropriate to the dynamic collective model, we chose to study nuclei around mass 100. It was found that ^{92}Mo and ^{96}Mo offered a reasonable test of the qualitative predictions of the dynamic collective model, namely that the inelastic scattering strength should be stronger for a nucleus which was soft against quadrupole vibrations. Calculations due to Arenhovel and Hayward[8] indicate that for ^{92}Mo, a very stiff rotator, inelastic scattering should be very weak while ^{96}Mo, a much softer vibrator, would show inelastic scattering to the first 2^+ state roughly 4— 5 times as strong. Figure 11 shows our measurements at 90° for the ^{92}Mo target together with the best two-Lorentzian fit. Within error, no inelastic scattering was observed for ^{92}Mo. The elastic scattering cross section was fit by a reasonable combination of resonance parameters for two Lorentzians. The data for ^{96}Mo is indicated in Fig. 12 together with a single Lorentzian fit to the elastic scattering and a corresponding fit to the inelastic scattering. A two Lorentzian fit did not give significant improvement over the one Lorentzian curve. There are two features of the inelastic scattering which are noteworthy in ^{96}Mo. First, again the inelastic scattering appears to be weaker than expected on the basis of the trends shown in the calculations using the dynamic collective model. Secondly, the inelastic scattering observed is more localized than a one Lorentzian fit would allow. Thus, while the data on the ^{92}Mo and ^{96}Mo are not quantitatively in agreement with the dynamic collective model, the trends do indicate that as the vibrator becomes softer the inelastic scattering is correspondingly stronger in agreement with prediction.

In conclusion, we have observed that coupling to surface vibrations in the giant dipole resonance is much weaker than the dynamic

collective model suggests. Second, the elastic scattering cross section in all targets but ^{60}Ni shows structure which is not evident in the absorption cross section measurement. It is evident that a substantial theoretical effort will be necessary to refine models of the interaction in order to explain the present results. One possibility will be to use dynamic collective model codes perhaps with more realistic resonance parameters in order to obtain satisfactory fits to the data. A second possibility will be to consider more realistic models for generating the giant dipole state in this mass region and to use these more realistic approximations in calculations of the coupling to surface vibrations.

This research was supported under the auspices of the U. S. Department of Energy and the National Science Foundation.

TABLE I. Parameters obtained from a two Lorentzian analysis of photon scattering cross sections.

Nucleus	σ_a (mb)	Γ_a (MeV)	E_a	σ_b (mb)	Γ_b (MeV)	E_b	$\Gamma^a_{2^+}/\Gamma^a_{el}$	$\Gamma^b_{2^+}/\Gamma^b_{el}$
^{60}Ni	64	3.59	16.1	42	3.56	19.2	0.13	0.30
^{52}Cr	64	6.31	17.2	29	1.28	20.4	0.19	0.01
^{56}Fe*	52	4.33	16.8	46	4.09	20.1	0.64	0.13
^{92}Mo	178	4.02	16.5	67	4.42	20.1	—	—
^{96}Mo	162	5.13	15.8	—	—	—	0.20	—

*Based on LLL parameters for ^{55}Mn, UCRL-74546.

TABLE II. Integrated absorption cross sections corresponding to best fits to photon elastic scattering.

Nucleus	$\frac{\pi}{2}(\sigma_a\Gamma_a + \sigma_b\Gamma_b)$ (MeV-b)		$\frac{0.06NZ}{A}$
	scattering	absorption	
^{52}Cr	0.692	—	0.775
^{56}Fe	0.649[a]	—	0.836
^{60}Ni	0.595	0.680	0.896
^{92}Mo	1.588	1.052	1.376
^{96}Mo	1.305	1.747	1.418

[a]Adjusted parameters for ^{55}Mn taken from UCRL-74546.

REFERENCES

[1] See review of M. Danos, Lectures on Photonuclear Physics, Univ. of Maryland, Tech. Report 221, 1961 (unpublished).

[2] M. Danos and W. Greiner, Phys. Rev. 134, B284 (1964); H. Arenhovel, G. Gneuss and V. Rezwani, Phys. Lett. 39B, 249 (1971).

[3] H. E. Jackson and K. J. Wetzel, Phys. Rev. Lett. 28, 513 (1972).

[4] J. S. O'Connell, et al., Phys. Rev. 126, 228 (1962).

[5] A. Kerman and H. K. Quang, Phys. Rev. 135, B883 (1964).

[6] H. Arenhovel and H. J. Weber, Nucl. Phys. 91, 145 (1967).

[7] H. E. Jackson and K. H. Wetzel, Phys. Rev. Lett. 28, 513 (1972).

[8] H. Arenhovel and E. Hayward, Phys. Rev. 165, 1170 (1968).

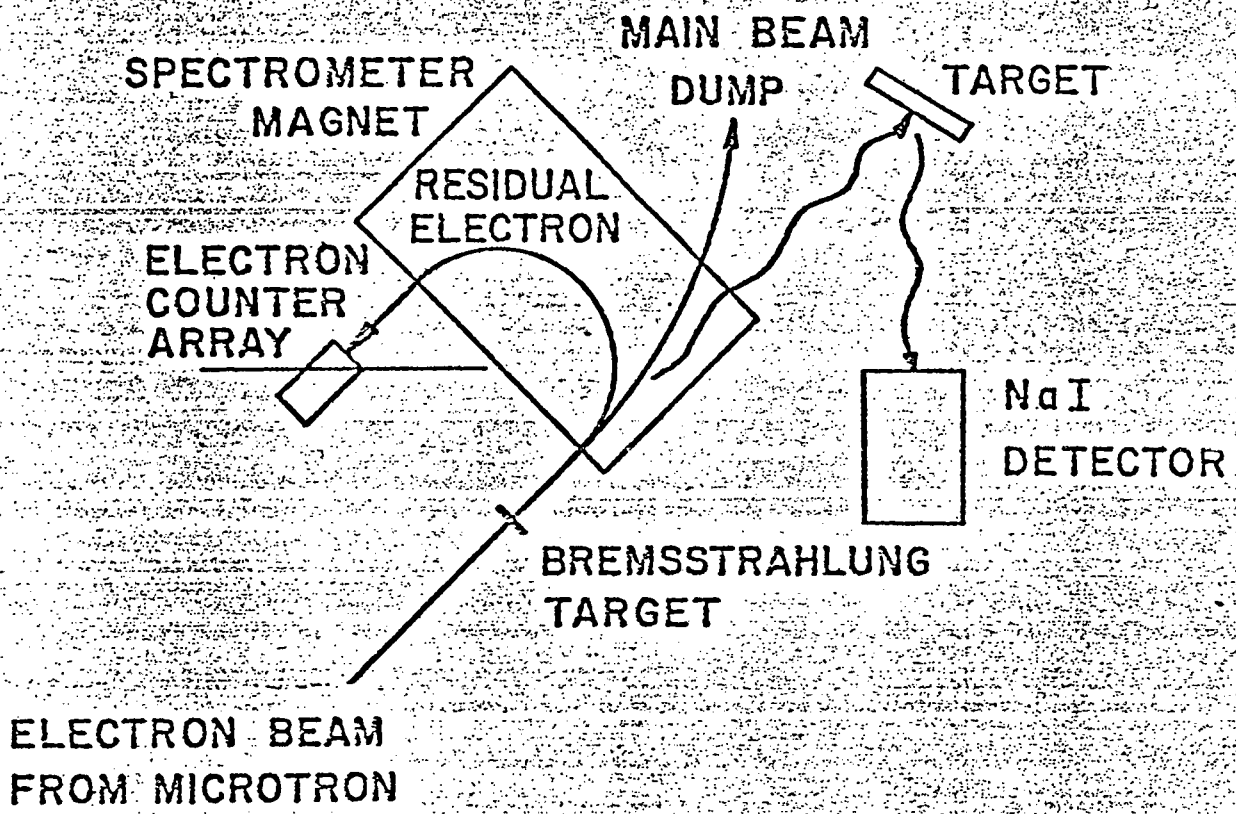

Fig. 1

259-78-267

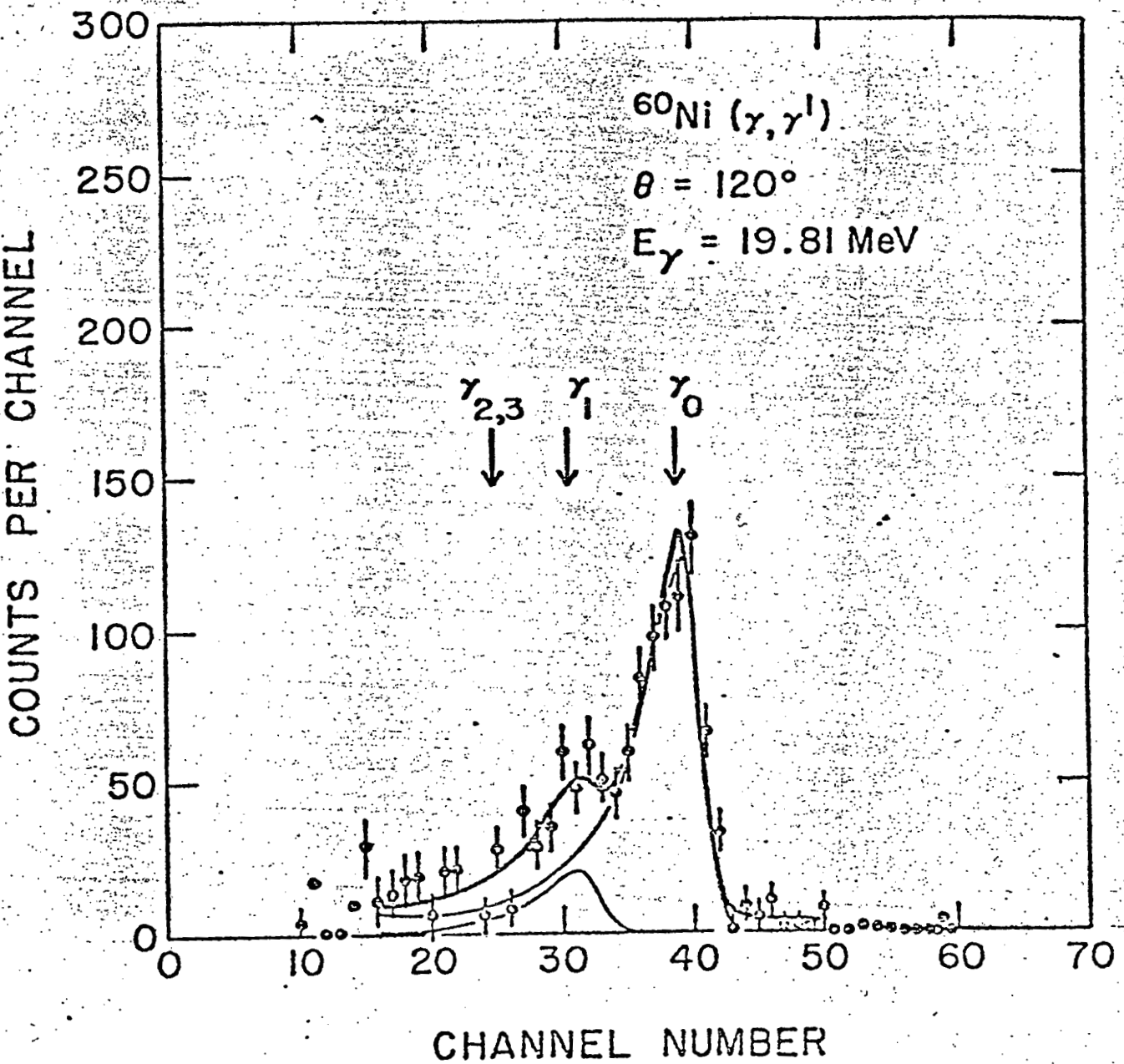
$^{60}Ni\ (\gamma,\gamma')$
$\theta = 120°$
$E_\gamma = 19.81$ MeV
$\gamma_{2,3}$
γ_1
γ_0
COUNTS PER CHANNEL
CHANNEL NUMBER
0
50
100
150
200
250
300
0
10
20
30
40
50
60
70

Figure 2

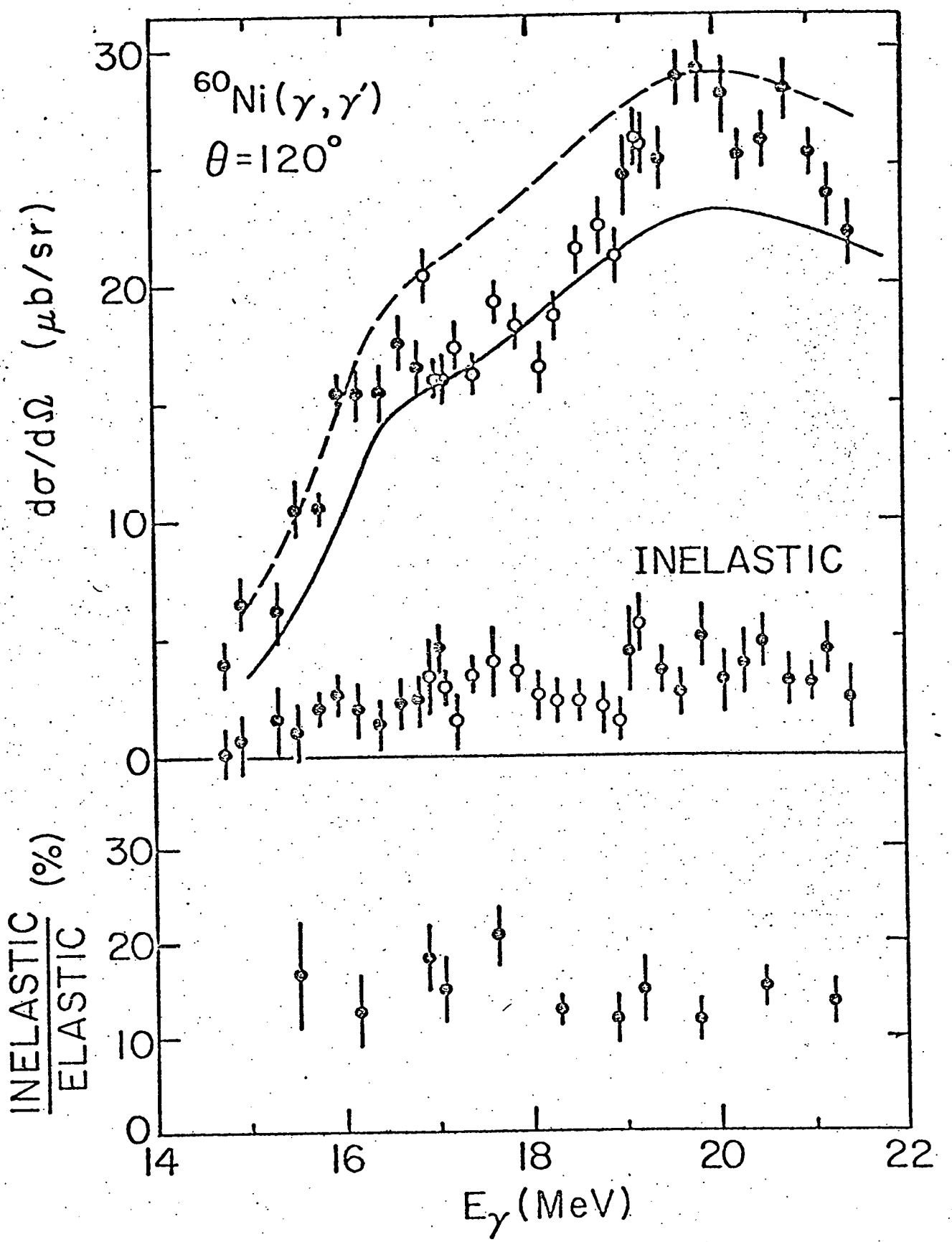
$^{60}Ni(\gamma,\gamma')$
$\theta=120°$
$d\sigma/d\Omega$ (μb/sr)
INELASTIC
$\frac{\text{INELASTIC}}{\text{ELASTIC}}$ (%)
E_γ (MeV)
30
20
10
0
30
20
10
0
14
16
18
20
22

Fig. 3

Fig. 12

$^{60}Ni(\gamma,\gamma)$ with & without Thomson Scattering

Fig. 5

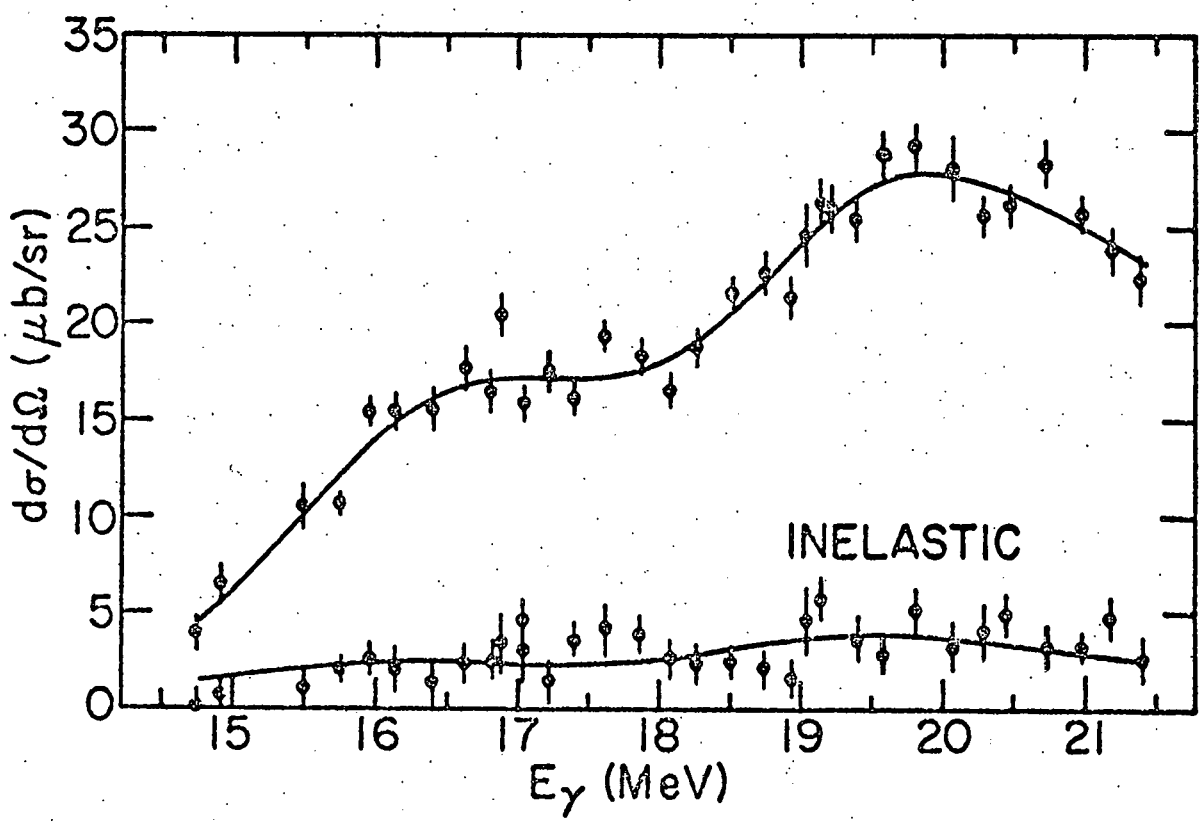

$^{60}Ni(\alpha,\alpha')$

Phy-15,172
3-23-79
D.K.

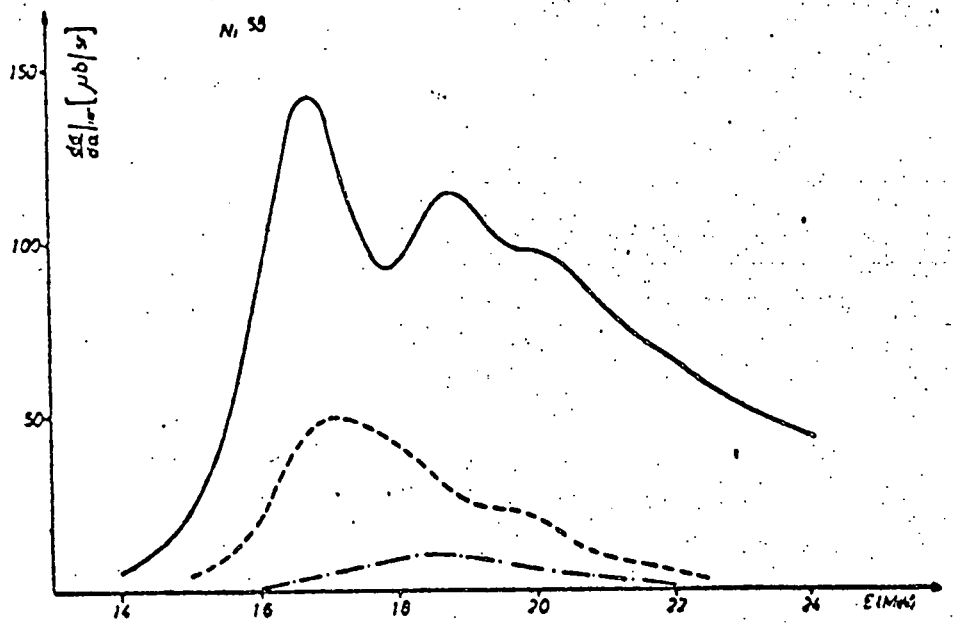

Fig. 5. Theoretical elastic (full curve) and inelastic (to first 2^+ state (dashed curve), to second 2^+ state (dot-and-dash curve)) scattering cross sections of ^{58}Ni.

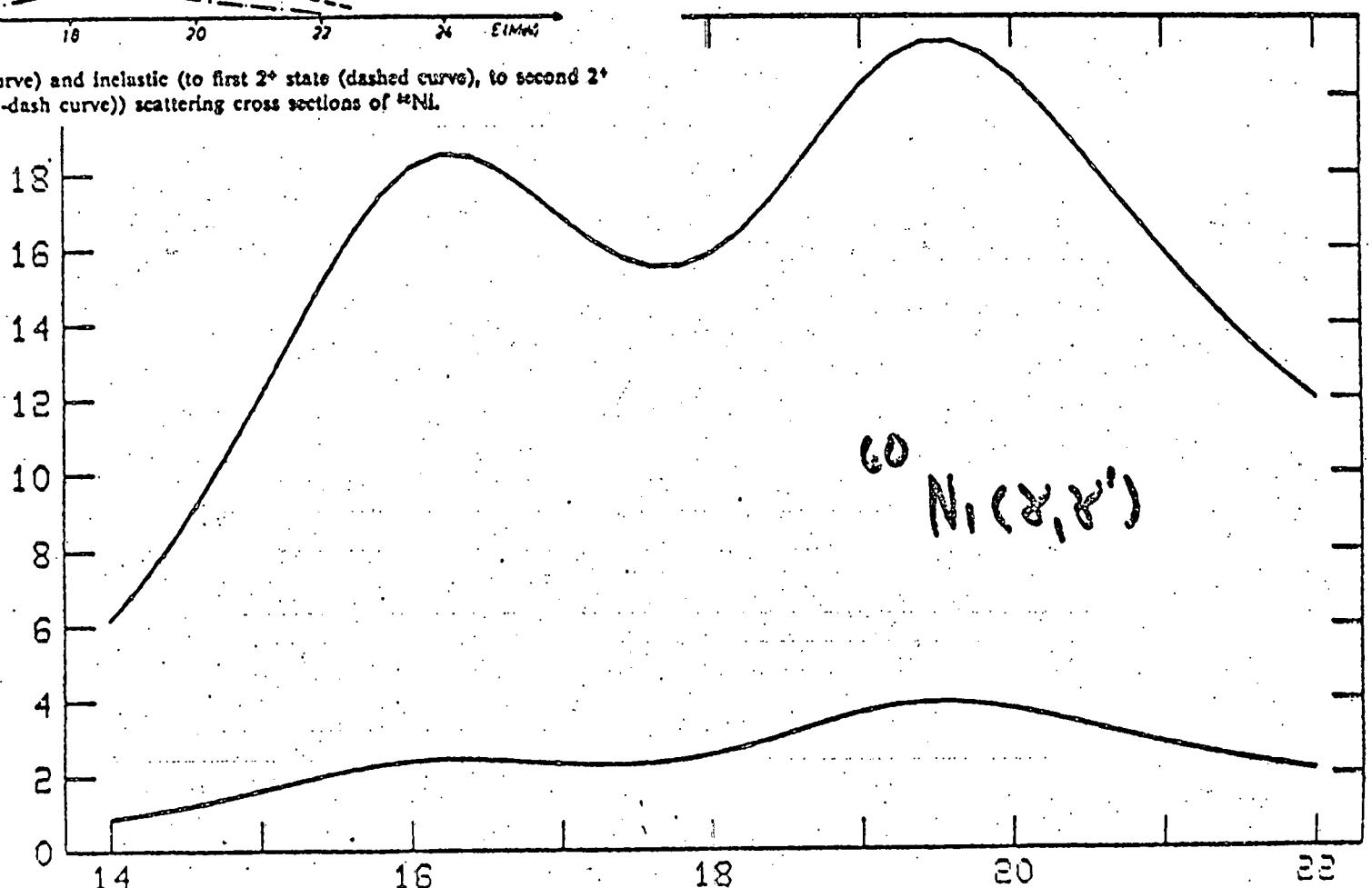

$^{52}Cr(\gamma,\gamma')$

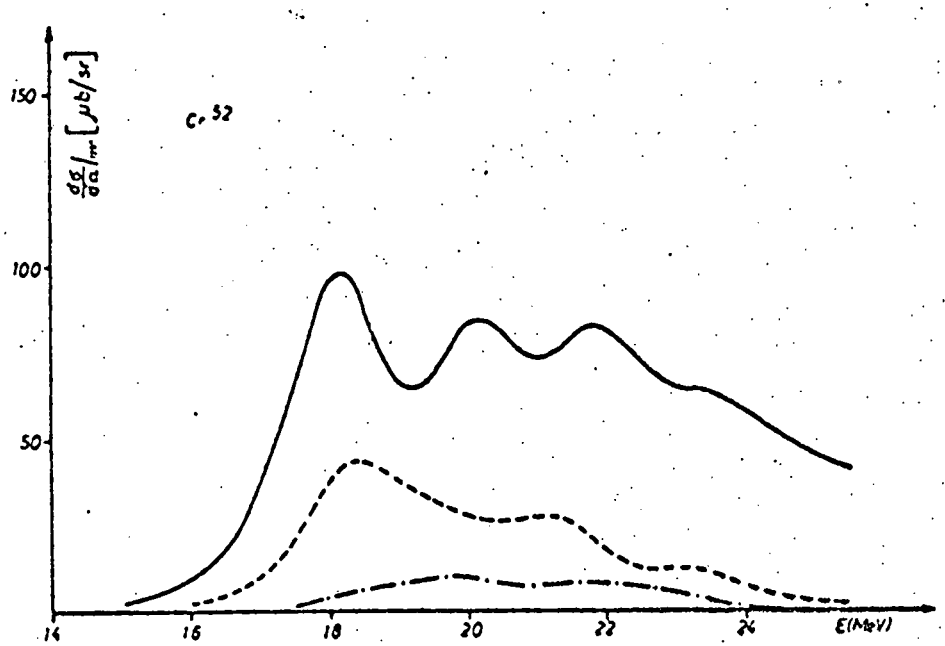

Fig. 3. Theoretical elastic (full curve) and inelastic (to first 2^+ state (dashed curve), to second 2^+ state (dot-and-dash curve)) scattering cross sections of ^{52}Cr.

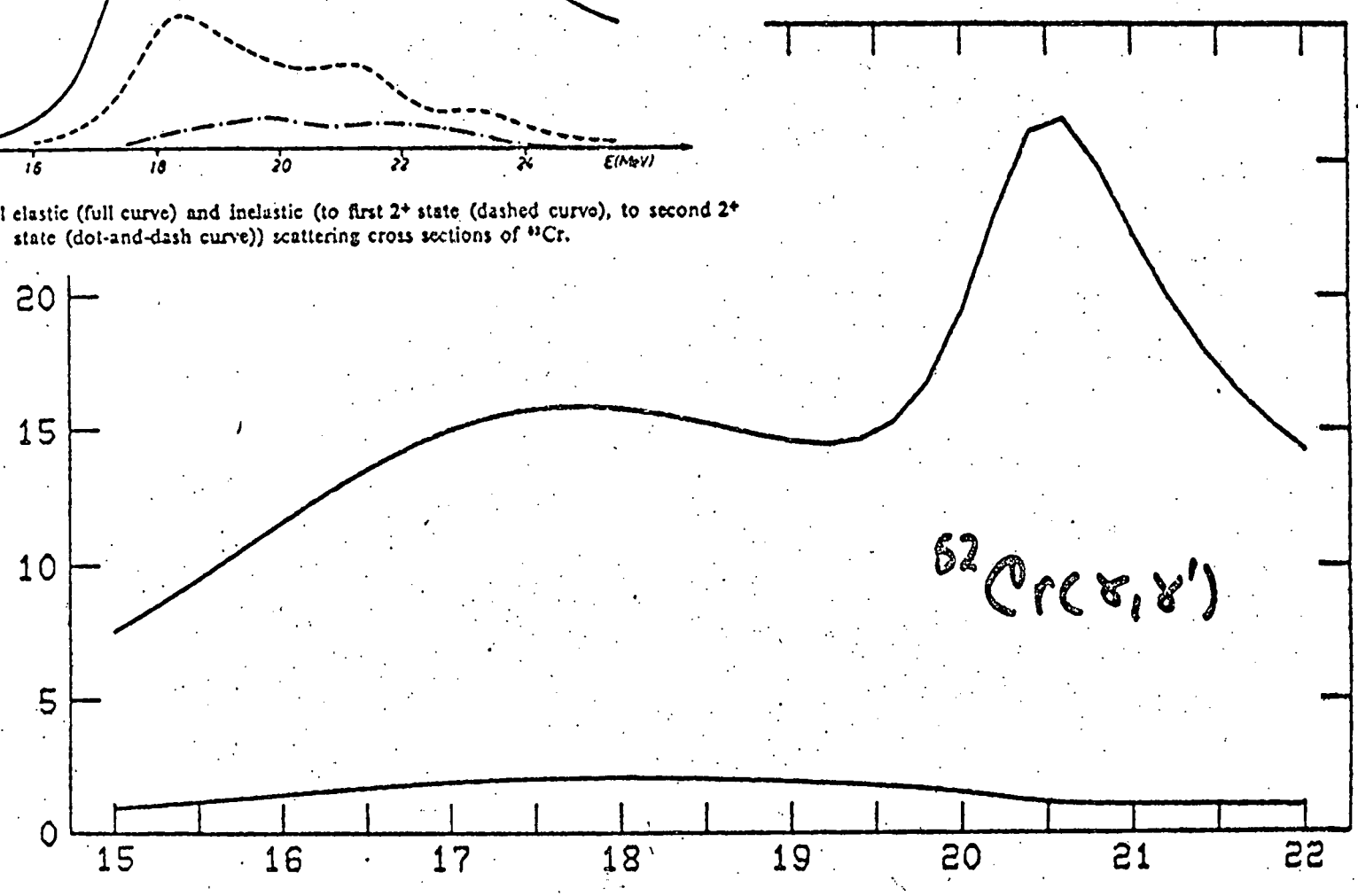

$^{56}Fe\ (\gamma, \gamma')$

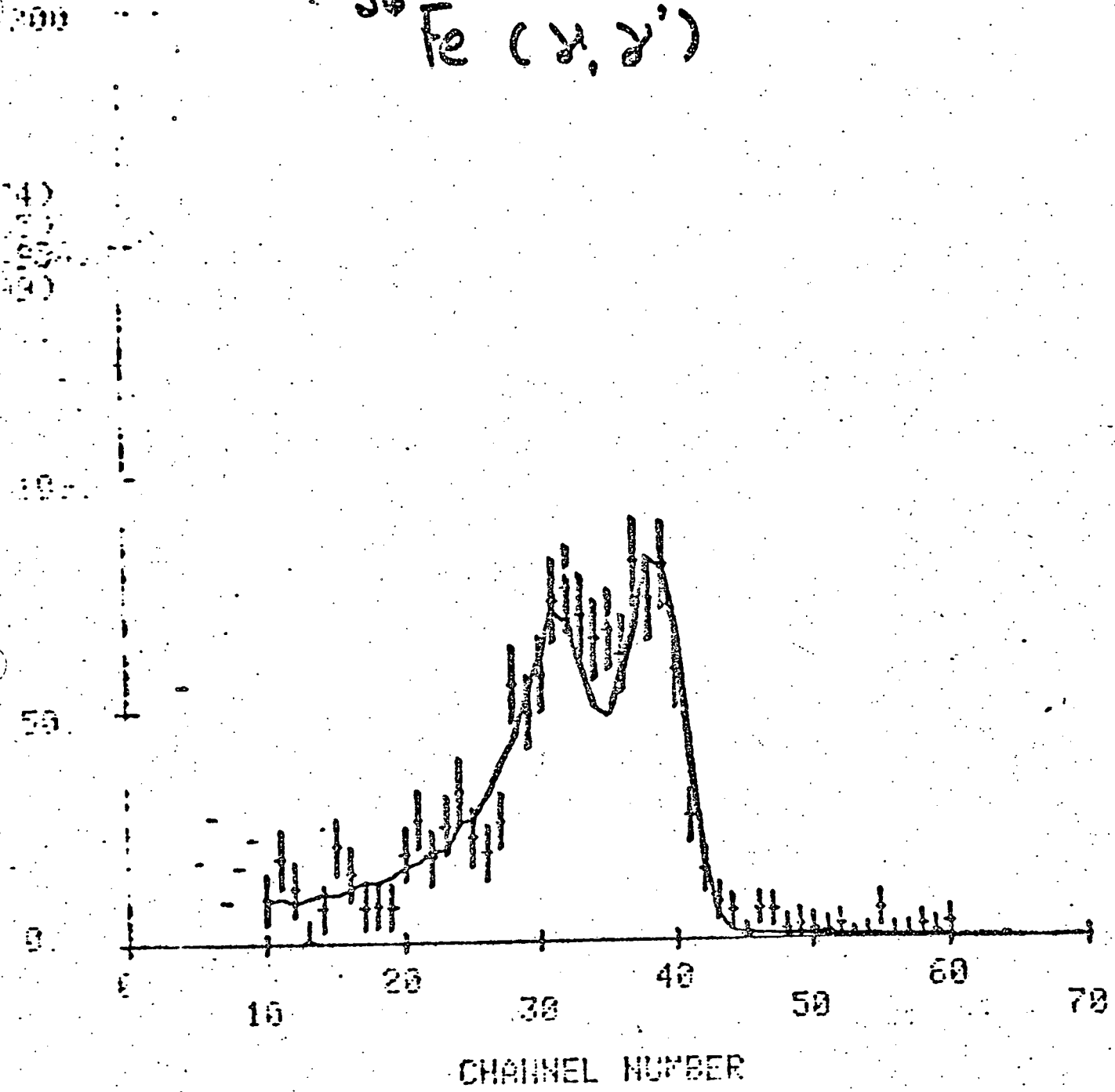

Fig. 9

Fig. 10

Fig. 11

شکل ۱۲